particular details of the 2DCO state may be material dependent, there appears to be a general correspondence between the broad and nested antinodal FS segments observed by ARPES and the propensity for 2D charge ordering in the lightly doped cuprates.

One recent intriguing model proposed for the 2DCO is a Wigner crystal (WC), whose formation is driven by the Coulomb repulsion between the doped holes (*24*). Although 2D WCs or 1D stripes provide appealing real-space visualizations, addressing the nodal states in a fundamental manner may prove difficult for these models. For the simple WC picture, virtually all holes should be locked into an insulating superlattice and the low-energy QPs arise from the overflow or deficit of holes away from certain favored commensurate dopings. On the other hand, in $La_{2-x}Sr_xCuO_4$ it has been argued that the nodal states may arise from disordered stripes (*25*). In both cases, the nodal states arise more as model-dependent byproducts, not fundamental constituents of the charge-ordered state.

On the other hand, it has long been known that CDW formation and SC are competing instabilities in a wide variety of materials (*26*). This is not entirely surprising, given that the same attractive effective interactions, typically electron-phonon, can give rise to both states in many materials. In the case of Na-CCOC, both *d*-SC and 2DCO appear to compete for the antinodes, and the strength of one order parameter should come at the expense of the other. For instance, although $Ca_{2-x}Na_xCuO_2Cl_2$ is a rather poor high-T_c SC, it exhibits very prominent modulations in the STM *dI*/*dV* maps. On the other hand, $Bi_2Sr_2CaCu_2O_{8+\delta}$ is one of the better high-T_c superconductors (maximum T_c = 96 K), but exhibits far less pronounced charge-density modulations at low energies (*21*–*23*). Along these lines, it is also possible that critical fluctuations between the 2DCO and another ordered state could result in the incoherent antinodal states (*27*), although it is not evident whether the nodal QPs would still remain well defined. A related possibility is that the 2DCO does not represent a CDW of single holes, but instead represents a density wave of preformed *d*-wave Cooper pairs or a pair density wave (PDW) (*28*).

Another potential explanation for the broad antinodal features may come from models based on Franck-Condon broadening, which have been proposed to describe the unusual spectral features in both the lightly doped cuprates (*29*, *30*) and the manganites (*31*), and may therefore explain the similarity of the high-energy pseudogaps found in the both systems. In such a scenario, the strong coupling of the electrons to any bosonic excitations would result in $Z \ll 1$, and spectral weight is transferred to incoherent, multiboson excitations. The high-energy pseudogap behavior in both the cuprates and manganites may then originate from the broad, suppressed tail of incoherent spectral weight, which obscures the very small, but possibly finite coherent QP. The apparently vertical dispersion in the antinodal regime can then be explained as originating not from a real QP band, but rather from this largely incoherent, pseudogapped spectral weight. In this picture, an effective anisotropic coupling could lead to a larger Z (weaker coupling) along the nodal direction and a much smaller, yet still finite Z, at the antinodes (strong coupling). However, this coupling alone may not be sufficient to cause the 2DCO, and it may be the combination of strong coupling and FS nesting which ultimately stabilizes the antinodal charge-ordered state.

Although Na-CCOC may provide the clearest case for relating real-space charge ordering to the anisotropy of electronic states in momentum space, we believe that this is indicative of a generic tendency of the cuprate superconductors. Irrespective of the microscopic model, the dichotomy between the sharp nodal QPs and broad antinodal states suggests the importance of strongly momentum-anisotropic interactions in Na-CCOC and places important restrictions on possible theoretical descriptions of the charge-ordered state and pseudogap phase.

References and Notes

1. T. Timusk, B. Statt, *Rep. Prog. Phys.* **62**, 61 (1999).
2. I. Affleck, J. B. Marston, *Phys. Rev. B* **37**, 3774 (1988).
3. J. Zaanen, O. Gunnarsson, *Phys. Rev. B* **40**, 7391 (1989).
4. J. M. Tranquada *et al.*, *Nature* **375**, 561 (1995).
5. V. J. Emery, S. A. Kivelson, H. Q. Lin, *Phys. Rev. Lett.* **64**, 475 (1990).
6. T. Hanaguri *et al.*, *Nature* **430**, 1001 (2004).
7. Y. Kohsaka *et al.*, *J. Am. Chem. Soc.* **124**, 12275 (2002).
8. K. Waku *et al.*, *Phys. Rev. B* **70**, 134501 (2004).
9. L. F. Mattheiss, *Phys. Rev. B* **42**, 354 (1990).
10. The observed discrepancy between the nominal Na composition and the area enclosed in the contours shown in Fig. 1, C and D, could imply that the experimentally extracted contours may not represent a true FS in the strict Fermi liquid sense, possibly because of the broad antinodal excitations.
11. A. Damascelli, Z. Hussain, Z.-X. Shen, *Rev. Mod. Phys.* **75**, 473 (2003).
12. D. S. Dessau *et al.*, *Phys. Rev. Lett.* **66**, 2160 (1991).
13. D. H. Lu *et al.*, *Phys. Rev. Lett.* **86**, 4370 (2001).
14. T. Yoshida *et al.*, *Phys. Rev. Lett.* **91**, 027001 (2003).
15. X. J. Zhou *et al.*, *Phys. Rev. Lett.* **92**, 187001 (2004).
16. V. Brouet *et al.*, *Phys. Rev. Lett.* **93**, 126405 (2004).
17. T. Nakagawa *et al.*, *Phys. Rev. B* **67**, 241401 (2003).
18. Y.-D. Chuang, A. D. Gromko, D. S. Dessau, T. Kimura, Y. Tokura, *Science* **292**, 1509 (2001).
19. M. B. Salamon, M. Jaime, *Rev. Mod. Phys.* **73**, 583 (2001).
20. Y. Ando, A. N. Lavrov, S. Komiya, K. Segawa, X. F. Sun, *Phys. Rev. Lett.* **87**, 017001 (2001).
21. M. Vershinin *et al.*, *Science* **303**, 1995 (2004).
22. J. E. Hoffman *et al.*, *Science* **295**, 466 (2002).
23. K. McElroy *et al.*, in preparation; preprint available at http://arxiv.org/cond-mat/0404005.
24. H. C. Fu, J. C. Davis, D.-H. Lee, in preparation; preprint available at http://arxiv.org/cond-mat/0403001.
25. M. I. Salkola, V. J. Emery, S. A. Kivelson, *Phys. Rev. Lett.* **77**, 155 (1996).
26. A. M. Gabovich, A. I. Voitenko, J. F. Annett, M. Ausloos, *Supercond. Sci. Technol.* **14**, R1 (2001).
27. S. Sachdev, *Science* **288**, 475 (2000).
28. H.-D. Chen, O. Vafek, A. Yazdani, S.-C. Zhang, *Phys. Rev. Lett.* **93**, 187002 (2004).
29. A. S. Mishchenko, N. Nagaosa, *Phys. Rev. Lett.* **93**, 036402 (2004).
30. K. M. Shen *et al.*, *Phys. Rev. Lett.* **93**, 267002 (2004).
31. V. Perebeinos, P. B. Allen, *Phys. Rev. Lett.* **85**, 5178 (2000).

32. We thank N. P. Armitage, H.-D. Chen, A. Damascelli, J. C. Davis, T. P. Devereaux, H. Eisaki, T. Hanaguri, J. P. Hu, D.-H. Lee, N. Nagaosa, T. Sasagawa, O. Vafek, S. C. Zhang, and X. J. Zhou for enlightening discussions. Stanford Synchrotron Radiation Laboratory is operated by the Department of Energy Office of Basic Energy Science under contract DE-AC03-765F00515. K.M.S. acknowledges Stanford Graduate Fellowships and Natural Sciences and Engineering Research Council of Canada for their support. The ARPES measurements at Stanford were also supported by NSF DMR-0304981 and Office of Naval Research N00014-98-1-0195.

3 August 2004; accepted 30 December 2004
10.1126/science.1103627

Asynchronous Bends in Pacific Seamount Trails: A Case for Extensional Volcanism?

Anthony A. P. Koppers* and Hubert Staudigel

The Gilbert Ridge and Tokelau Seamounts are the only seamount trails in the Pacific Ocean with a sharp 60° bend, similar to the Hawaii-Emperor bend (HEB). These two bends should be coeval with the 47-million-year-old HEB if they were formed by stationary hot spots, and assuming Pacific plate motion only. New $^{40}Ar/^{39}Ar$ ages indicate that the bends in the Gilbert Ridge and Tokelau seamount trail were formed much earlier than the HEB at 67 and 57 million years ago, respectively. Such asynchronous bends cannot be reconciled with the stationary hot spot paradigm, possibly suggesting hot spot motion or magmatism caused by short-term local lithospheric extension.

The Hawaii-Emperor island and seamount chain is the most prominent morphologic feature on the seafloor, with a sharp 60° change in azimuth, called the Hawaii-Emperor bend (HEB). The HEB serves as a textbook example of the fixed hot spot hypothesis, in

which changes in the azimuth of volcanic lineaments are explained by changes in plate motion, and the hot spots that created these volcanoes remain fixed beneath the moving tectonic plates. Recent suggestions that the HEB was formed by a combination of plate and hot spot motion (*1*, *2*) weaken the fixed hot spot hypothesis, undermining the direct use of seamount trends and the age progressions therein for determining absolute plate-motion vectors. We studied two other HEB-type bends in the Pacific to understand the underlying causes of such azimuthal changes in intraplate volcanic lineaments. These bends can be found at the southern ends of the Gilbert Ridge and Tokelau seamount trail (Fig. 1) that recently were attributed to a group of now-extinct hot spots in the central Pacific Ocean (*3*, *4*), even though volcanism in these chains terminated shortly after the bends formed. The Louisville seamount trail is not useful for an independent age constraint of the HEB, because it shows only a very broad curvature at its bend (*5*).

We explored and dredged the Gilbert Ridge and Tokelau seamount trail aboard the research vessel *R/V Melville* and dated the dredged samples using the $^{40}Ar/^{39}Ar$ dating technique. Our dredging targeted deep volcanic features at the base of these seamounts, and we recovered mostly volcanic materials from which we dated acid-leached groundmass separates (*6*, *7*), or plagioclase, hornblende, and biotite mineral phases (Table 1). The results of our dating study are plotted on the maps in Fig. 2, where we compare the actual $^{40}Ar/^{39}Ar$ age distribution to the predicted plate-motion vectors and seamount ages along the Gilbert Ridge and Tokelau seamount trail from the most recent Pacific plate-motion models (*3*, *4*). These models suggest that the northern and southern parts of the Tokelau seamount trail were formed by two currently inactive hot spots located 5° and 11° to the north of Mcdonald hot spot, whereas the Gilbert Ridge is a composite seamount trail related to three hot spots located 1°, 5°, and 9° north of the Cook-Austral islands. However, our data show that the HEB-type bends in both locations were not formed at 47 million years ago (Ma), as assumed in these models, but rather around 67 Ma for the Gilbert Ridge and 57 Ma for the Tokelau seamount trail. The asynchronous timing of these HEB-type bends causes us to reject the idea that they originated from a group of fixed hot spots and requires us to explore other models for the development of bends in seamount trails. Three alternate models may explain the asynchronous timing of these bends: (i) decelerating motion of hot spot plumes, (ii) channeling of magma away from the hot spots, and (iii) extension of the Pacific plate caused by short-term changes in local plate stresses.

Decelerating motion of hot spots may produce similarly appearing bends asynchronously, in particular, when short-lived mantle plumes terminate magma production and become stationary during their final ascent through a more viscous upper mantle. Hot spot motion is inherent to large-scale mantle convection, where buoyant mantle plumes may shift from fixed and vertically straight positions to tilted positions that are not anchored in the deep mantle (*8*–*10*). The Hawaiian hot spot may have displayed such behavior between 80 and 47 Ma, when it experienced a north-to-south motion at 44 mm/year (*2*, *11*). In this scenario, the NNW Emperor seamount trail azimuth reflects the vector sum of this hot spot motion and a constant plate motion to the NW over the past 80 million years. A considerable slowing of the Hawaiian hot spot around 47 Ma would gradually change the azimuth of its hot spot track toward the northwestern azimuth of Pacific plate motion, as reflected in the Hawaiian seamount trail (*1*, *11*, *12*). Such a deceleration from a south-moving hot spot may also explain the origin of the Gilbert Ridge and Tokelau HEB-type bends, with a termination of hot spot motion around 67 and 57 Ma, respectively. Although this model clearly offers a potential mechanism, there are some problems with it as well. In particular, this model requires two closely spaced small-scale mantle plumes with very consistent hot spot motions for some time, but rapid deceleration and termination at different times, which appear

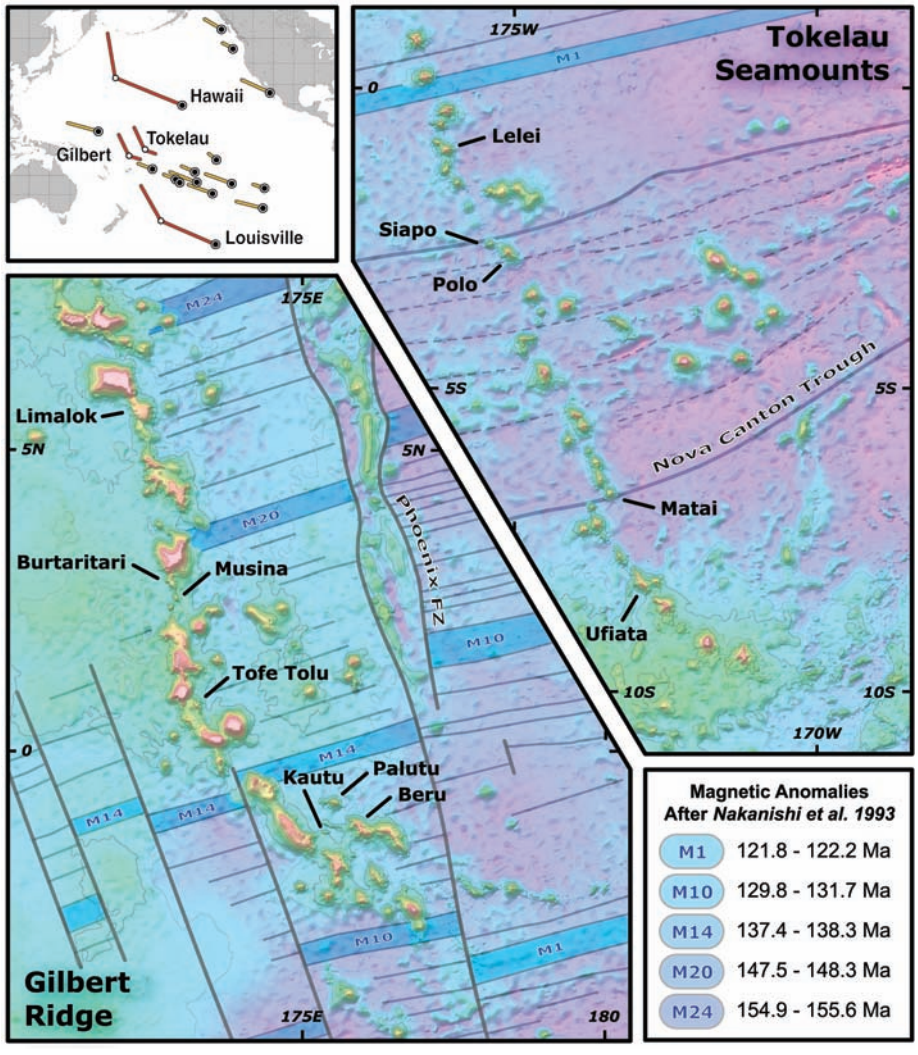

Fig. 1. Bathymetric maps for the Gilbert Ridge and Tokelau seamount trails based on a combination of multibeam data from the AVON Leg 2 cruise onboard the *R/V Melville* and global predicted bathymetry (*17*). Magnetic anomalies and fracture zones in the underlying Pacific oceanic crust (*18*) have been indicated to highlight the lithospheric structure of the Pacific plate. See Table 1 for Web links to the Seamount Catalog for multibeam data, grids, and detailed bathymetric seamount maps.

Institute of Geophysics and Planetary Physics, Scripps Institution of Oceanography, University of California, San Diego, La Jolla, CA 92093–0225, USA.

*To whom correspondence should be addressed. E-mail: akoppers@ucsd.edu

unlikely in the same local mantle-convection regime. In addition, the Gilbert Ridge shows ages predominantly in the range between 69 and 65 Ma, suggesting very rapid hot spot motion on the order of 130 mm/year, a velocity that is well beyond the average (~10 mm/year) hot spot motions that are predicted in numerical mantle flow models (*13*).

At first sight, the rather complex structure of the local seafloor (Fig. 1) makes magma diversion away from the main seamount trails a good option for explaining the southeastern deflections observed in the Gilbert Ridge and Tokelau seamount trail. However, a brief examination of the ocean floor structure makes this explanation the least likely among the three options discussed here. Both seamount trails were formed on 50- to 65-million-year-old oceanic crust but terminate in locations of relatively thick and cold lithosphere, just before plate motion would have moved thinner and more vulnerable lithosphere over the mantle plume upwellings. The Gilbert Ridge died out just before northwestern plate motion would decrease the age of the overriding lithosphere at the east side of the Phoenix transform fault, and the Tokelau chain terminated just as the eastern extension of the Manihiki plateau passed the region (Fig. 1). In both cases, we would expect that plume and magma channeling delivered materials very effectively to the thinner Pacific lithosphere, where it met much less resistance to magma transport.

Mantle upwelling caused by plate thinning and extension has been considered as another reason for the development of some seamount trails (*14*, *15*). Plate extension may be related to long-term and plate-wide processes because they are the result of the long-term subduction and ridge-push forces that determine the overall plate-motion vectors (*16*). They may also be short term (10^5 to 10^6 years) and/or localized in particular regions of a tectonic plate, without an apparent impact on the overall long-term plate-motion vector. The latter scenario may be caused by abrupt changes in the subduction zone force balance, because of the arrival of a weak zone that allows the crust to tear, or because of the arrival of an obstacle to subduction, such as a seamount trail or volcanic plateau. As a result, slab-pull forces may change for short durations, causing extensional volcanism at preexisting zones of weakness that are reactivated by minor local changes in plate stress. The stress field will return to its previous state as soon as the subduction zone forces return to their original configuration. We propose that the southwestern Pacific plate experienced two such short-term extensional phases, one around 67 Ma and one around 57 Ma, possibly reactivating the inactive spreading center that formed the Nova Canton Trough and reactivating seafloor preconditioned by small-volume intraplate volcanism that formed close to this ancient Pacific spreading center around 115 Ma and crosses the Phoenix fracture zone to its east. The Tokelau chain also displays a deflection from its NNW azimuth at 3°S, resulting in offshoots that are similar to the bend at its southern termination. This bend may have formed at the same time as the Gilbert Ridge bend, offering independent support for the 67-Ma phase of local plate extension. Overall, plate extension is the strongest alternative among our three options, but there are very few arguments or clues that positively identify any particular explanation.

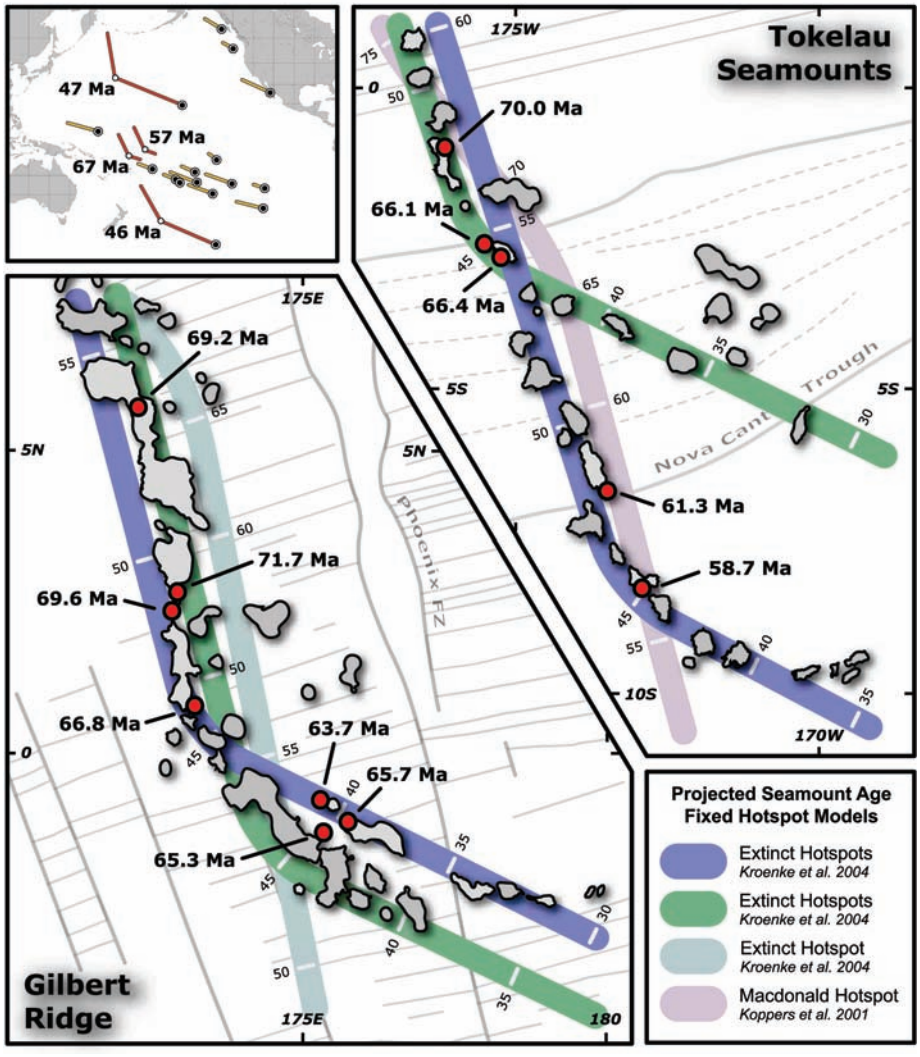

Fig. 2. Average seamount ages based on $^{40}Ar/^{39}Ar$ analyses with respect to the predicted plate motion between 30 and 80 Ma, based on the most recent models from Wessel and Kroenke (*3*, *4*) and assuming fixed hot spots. One prediction by the plate-motion model of Koppers *et al*. 2001 (*19*) for Macdonald hot spot is shown for comparison reasons. All ages are in Ma and are listed in Table 1. The 69.2-Ma age for Limalok guyot was previously published in Koppers *et al*. 2000 (*7*) but has been recalibrated here to reflect the 28.04-Ma Fish Canyon Tuff (FCT-3) biotite age standard.

Our findings influence our views of oceanic intraplate volcanism and absolute Pacific plate motion: (i) The textbook explanation for intraplate volcanism by fixed hot spots is either entirely wrong or insufficient to explain these phenomena. (ii) Hot spots are likely not to be stationary, but move with the convecting mantle. (iii) Non–hot spot/plume models have to be considered for explaining intraplate volcanism, whereby local lithospheric extensions are likely to be an important candidate. (iv) Furthermore, absolute Pacific plate motion, for the time period between 80 and 47 Ma, is extremely poorly constrained. It is not clear if any of the three HEB-type bends on the Pacific plate are caused by a change in plate-motion direction, and it is similarly uncertain if the plate moved NW (along an extended Hawaiian trend) or NNW as indicated by the Emperor seamount trail.

References and Notes

1. I. O. Norton, *Tectonics* **14**, 1080 (1995).
2. J. A. Tarduno *et al.*, *Science* **301**, 1064 (2003).
3. P. Wessel, Y. Harada, L. W. Kroenke, A. Sterling, *Eos* **84**, V32A (2003).

Table 1. Gilbert Ridge and Tokelau Seamounts argon geochronology. Average $^{40}Ar/^{39}Ar$ ages for seamounts in the Gilbert Ridge and Tokelau seamount trails are given. All samples were monitored against Fish Canyon Tuff (FCT-3) biotite (28.04 ± 0.18 Ma) as calibrated by Renne *et al*. (*20*). Reported errors on the $^{40}Ar/^{39}Ar$ ages are on the 95% confidence level, including 0.3 to 0.4% standard deviation on the neutron flux correction factor, or *J* value. All input parameters to the calculations are published in table 2 of Koppers *et al*. (*21*), whereas the ArArCALC v2.2 age calculations are described in Koppers (*22*). Visit the Seamount Catalog at http://earthref.org to find detailed bathymetric maps, grid files, and the multibeam data from the AVON Leg 2 cruise onboard the *R/V Melville* of the Scripps Institution of Oceanography. Use the catalog number in the last column of this table to generate links such as http://earthref.org/cgi-bin/sc.cgi?id=SMNT-067S-1734W that will guide you to the index pages of each dated seamount.

Seamount name	Latitude	Longitude	Age ± 2σ (Ma)	*n*	EarthRef.org Seamount Catalog index number
		Gilbert Ridge			
Burtaritari	2°41.9′N	172°48.2′E	71.7 ± 0.4	2	SMNT-032N-1729E
Musina	2°29.3′N	172°51.7′E	69.6 ± 0.6	2	SMNT-025N-1729E
Tofetolu	0°46.8′N	173°16.1′E	66.8 ± 0.5	2	SMNT-007N-1733E
Palutu	0°55.0′S	175°29.0′E	63.7 ± 0.5	1	SMNT-009S-1755E
Beru	1°08.5′S	175°43.7′E	65.7 ± 0.7	1	SMNT-013S-1760E
Kautu	1°20.8′S	175°20.6′E	65.3 ± 0.5	2	SMNT-014S-1754E
		Tokelau Seamounts			
Lelei	1°04.4′S	176°11.5′	70.0 ± 0.5	3	SMNT-010S-1761W
Siapo	2°36.2′S	175°25.0′	66.1 ± 0.6	4	SMNT-026S-1754W
Polo	2°46.9′S	175°09.0′	66.4 ± 0.6	2	SMNT-027S-1751W
Matai	6°41.9′S	173°28.0′	61.3 ± 0.6	2	SMNT-067S-1734W
Ufiata	8°16.3′S	172°52.7′	58.4 ± 0.3	2	SMNT-082S-1729W

4. L. W. Kroenke, P. Wessel, A. Sterling, in *Origin and Evolution of the Ontong Java Plateau*, J. G. Fitton, J. J. Mahoney, P. J. Wallace, A. D. Saunders, Eds. (Geological Society of London, London, 2004), vol. 229, pp. 9–20.
5. P. Lonsdale, *J. Geophys. Res.* **93**, 3078 (1988).
6. A. A. P. Koppers, H. Staudigel, M. S. Pringle, J. R. Wijbrans, *Geochem. Geophy. Geosyst.* **4**, 1089 (2003).
7. A. A. P. Koppers, H. Staudigel, J. R. Wijbrans, *Chem. Geol.* **166**, 139 (2000).
8. B. Steinberger, R. J. O'Connell, *Geophys. J. Int.* **132**, 412 (1998).
9. B. Steinberger, *J. Geophys. Res.* **105**, 11127 (2000).
10. J. P. Lowman, S. D. King, C. W. Gable, *Geochem. Geophys. Geosyst.* **5**, Q01L01 (2004).
11. R. A. Duncan, R. A. Keller, *Geochem. Geophys. Geosyst.* **5**, Q08L03 (2004).
12. P. Molnar, J. Stock, *Nature* **327**, 587 (1987).
13. B. Steinberger, R. Sutherland, R. J. O'Connell, *Nature* **430**, 167 (2004).
14. E. L. Winterer, D. T. Sandwell, *Nature* **329**, 534 (1987).
15. D. T. Sandwell *et al.*, *J. Geophys. Res.* **100**, 15087 (1995).
16. C. Lithgow-Bertelloni, J. H. Guynn, *J. Geophys. Res.* **109**, B014108 (2004).
17. W. H. F. Smith, D. T. Sandwell, *Science* **277**, 1956 (1997).
18. M. Nakanishi, K. Tamaki, K. Kobayashi, *Geophys. J. Int.* **144**, 535 (1992).
19. A. A. P. Koppers, J. P. Morgan, J. W. Morgan, H. Staudigel, *Earth Planet. Sci. Lett.* **185**, 237 (2001).
20. P. R. Renne *et al.*, *Chem. Geol.* **145**, 117 (1998).
21. A. A. P. Koppers, H. Staudigel, R. A. Duncan, *Geochem. Geophys. Geosyst.* **4**, 8914 (2003).
22. A. A. P. Koppers, *Comput. Geosci.* **28**, 605 (2002).

23. We acknowledge funding from NSF Division of Ocean Sciences through grants NSF–OCE 9730394 and NSF-OCE 0002875. In particular, we express our appreciation of our long-term collaboration with R. A. Duncan and the use of his laboratory. This study was initiated through stimulating brainstorming with J. Phipps Morgan, and the dredging was supported by a group of superb shipmates, including K. Arbesman, J. Dodds, S. W. Herman, J. Konter, T. M. Lassak, J. Phipps Morgan, W. Sager, and R. Taylor. Any opinions, findings, and conclusions or recommendations expressed in this material are those of the authors and do not necessarily reflect the views of NSF.

8 November 2004; accepted 5 January 2005
10.1126/science.1107260

Liquid Carbon, Carbon-Glass Beads, and the Crystallization of Carbon Nanotubes

Walt A. de Heer,[1]* Philippe Poncharal,[2] Claire Berger,[3] Joseph Gezo,[4] Zhimin Song,[1] Jefferson Bettini,[5] Daniel Ugarte[5,6]

The formation of carbon nanotubes in a pure carbon arc in a helium atmosphere is found to involve liquid carbon. Electron microscopy shows a viscous liquid-like amorphous carbon layer covering the surfaces of nanotube-containing millimeter-sized columnar structures from which the cathode deposit is composed. Regularly spaced, submicrometer-sized spherical beads of amorphous carbon are often found on the nanotubes at the surfaces of these columns. Apparently, at the anode, liquid-carbon drops form, which acquire a carbon-glass surface due to rapid evaporative cooling. Nanotubes crystallize inside the supercooled, glass-coated liquid-carbon drops. The carbon-glass layer ultimately coats and beads on the nanotubes near the surface.

The original arc method to produce multiwalled carbon nanotubes (MWNTs) introduced by Ebbesen and Ajayan (*1*, *2*) was an extension of the pure carbon-arc production method for fullerenes developed by Krätschmer and Huffman (*3*). In this method, a pure (catalyst-free) carbon arc (100 A, 30 V) is struck between two carbon electrodes in a helium atmosphere. When the helium pressure is low ($P_{He} \sim 10$ mb), the arc emits a dense fullerene smoke; at higher pressures, carbon nanotubes are formed. In contrast to catalytically produced MWNTs, pure carbon-arc–produced MWNTs are essentially defect free. Here, we present evidence that pure carbon-arc–produced MWNTs form by homogeneous nucleation in liquid carbon, inside elongated carbon droplets coated with a thin layer of carbon glass.

Although the catalytic production process has been extensively studied, little is known about MWNT formation in pure arcs. Earlier proposed formation mechanisms can be classified in two categories. The vapor-growth mechanism involves growth of nanotubes on the cathode in a dense flux of carbon atoms in the arc. Several scenarios have been considered to explain the vapor-solid growth process that is at the same time consistent with the morphology of the nanotube deposits (*4*, *5*). Alternatively, it is known that nanotubes form by heat treatment of various carbonaceous materials (*6*, *7*), and solid-phase production of arc-produced nanotubes was inferred from these observations (*7*). While these mechanisms may indeed produce nanotubes under favorable circumstances, we show that pure carbon-arc–produced nanotubes are formed from a liquid precursor.

Ebbesen and Ajayan (*1*) discovered that when the helium pressure in the Krätschmer-Huffman carbon arc is increased so that $P_{He} >$ 100 mb, a 7-mm-diameter cylindrical carbonaceous deposit forms on the cathode at a rate of about 1 mm per min from a 7-mm-diameter anode. The core of the deposit consists of a basaltic structure of carbon columns parallel to the cylinder axis. The columns are about 1 mm long and about 0.1 mm wide (Fig. 1). They are mechanically stable and easily sepa-

[1]School of Physics, Georgia Institute of Technology, Atlanta, GA 30332, USA. [2]Université Montpellier 2 GDPC, Place Eugène Bataillon 34095 Montpellier, Cedex 5, France. [3]CNRS-LEPES, BP 166, 38042 Grenoble, Cedex 9, France. [4]University of Illinois at Urbana-Champaign, Department of Physics, 1110 West Green Street, Urbana, IL 61801, USA. [5]Laboratório Nacional de Luz Síncrotron, Caixa Postal 6192,13084-971 Campinas SP, Brazil. [6]Instituto de Física Gleb Wataghin, Universidade Estadual de Campinas, Caixa Postal 6165, 13083-970 Campinas SP, Brazil.

*To whom correspondence should be addressed. E-mail: walt.deheer@physics.gatech.edu